Evolution of particle structure during water sorption observed on different size fractions of durum wheat semolina

Ingrid Murrieta-Pazos, Laurence Galet, Severine Patry, Claire Gaiani, Joël Scher

Evolution of particle structure during water sorption observed on different size fractions of durum wheat semolina

Ingrid Murrieta-Pazos [a,b], Laurence Galet [a,*], Séverine Patry [a], Claire Gaiani [b], Joël Scher [b]

[a] Université de Toulouse, Mines Albi, Centre RAPSODEE, CNRS UMR 5302, Campus Jarlard, F-81013 Albi CT cedex 09, France
[b] Université de Lorraine, LIBio — Laboratoire d'Ingénierie des Biomolécules, 2 avenue de la Foret de Haye, TSA 40602, 54518 Vandoeuvre les Nancy, France

A B S T R A C T

This work examines the effect of the particle size of durum wheat semolina on the water diffusion coefficient and the evolution of the microstructure during hydration. Durum wheat semolina was sieved in 5 size categories. Water–particle interaction of powders (5 fractions and raw semolina) was studied using dynamic vapour sorption. Water sorption isotherms were fitted to G.A.B.. and Y&N models. Monolayer values as well as multilayer properties were calculated and compared. Absorption properties were determined by Y&N model. A sorption curve was modelled with the Fickian diffusion equation adapted to water diffusion into solid particles. A dynamic Fickian water diffusion coefficient was calculated for each particle size after conditioning at different RHs. The surface structure of conditioned fractions was observed by ESEM. The microstructure of semolina presented an evolution with the increase of size and RH. Starch grains presented an increased size and protein matrix had a different texture. After correlation of isotherm data and microstructure, the resulting state and properties of the components were a key to understand diffusion on food powder systems.

Keywords:
Food powder
Sorption isotherm
Microstructure
Semolina
Particle size
Water diffusion coefficient

1. Introduction

Durum wheat flour (semolina) is a raw material widely used in several processes such as the production of pasta or couscous. It is necessary to understand water transfer in these processes and during the storage of semolina to increase production efficiency and obtain quality products. This transfer can be limited by the surface properties of the particles, which significantly influences a number of functional properties, i.e. hydration, caking, agglomeration. Consequently the study of water transfer on the surface of particles is of relevance.

Water transfer using sorption isotherms of soft flours has been studied [1–3], only a few publications corresponding to semolina are available [4–6]. In addition there are few studies about water diffusion coefficients in flour particles [5,7].

The evolution of the microstructure with increasing water content may produce an increase of particle size as well as changes in the properties of components, thus diffusion can be affected. In this regard, the microstructural changes during the hydration of food powders have a great scientific interest for many practical applications For example, during milk reconstitution, the water transfer into the milk particles depends on the succession of the different reconstitution steps: wettability, sinkability, dispersibility and finally solubility of surface molecules. These steps depend on the nature and composition of the powder. In this context, changes on microstructure due to water sorption were studied by Murrieta-Pazos et al. [8]. These authors conditioned milk powder samples at different RH and observed the microstructure by ESEM. Despite the interest of such evolution this approach has not been applied to flour particles. The aim of this work was to study the effect of particle size on the water diffusion coefficient and the microstructural evolution throughout hydration of durum wheat semolina.

2. Materials and methods

2.1. Materials

Industrial semolina (Panzani, Marseille, France) was sieved into different size grades in decreasing mesh size (0, 160, 250, 315, 400, 500 μm) from top to bottom (Retsch, Germany). The operating conditions were chosen after a kinetic study of the sieving process. For this 400 g of powder was placed on the first sieve and sieved for 12 h with amplitude of 40 on the scale of the apparatus. These conditions were optimized to enhance fine particle separation. The powder remaining on the sieves was collected producing 5 fractions with a range of diameters (0–160, 160–250, 250–315, 315–400, 400–500 μm). The original powder (raw powder) was also used in the subsequent experiments.

Three of the size fractions (0–160, 250–315, 400–500 μm) were *pseudo*-equilibrated under different relative humidity at 25 °C for seven days in five hermetic vessels containing saturated salt solutions

Abbreviations: BET, Brunauer–Emmett–Teller model; GAB model, Guggenheim–Anderson–de Boer model; RH, relative humidity; ESEM, environmental scanning electron microscopy; SE, secondary electron; GES, gaseous secondary electron; Y&N model, Young and Nelson model; IUPAC, International Union of Pure and Applied Chemistry.

* Corresponding author. Tel.: +33 5 63 49 32 35; fax: +33 5 63 49 30 25.
E-mail address: Laurence.Galet@mines-albi.fr (L. Galet).

(Sigma-Aldrich) of known RH: 0.11 (LiCl); 0.54 $Mg(NO_3)_2$; 0.75 (NaCl); 0.85 (KCl) and 0.97 (K_2SO_4). In each vessel, one millilitre of toluene (recommended for non-fatty products) was placed in a separated recipient near to the samples in order to avoid the proliferation of microorganisms [9]. This process was performed to determine the change in size and microstructure of the particles under varying RH; however the fitting of the models as well as the calculation of diffusion coefficients was obtained using data from DVS, where humidity is truly equilibrated.

2.2. Bulk composition

Water content was measured by weight loss after drying at 105 °C. Ash content was also measured by weight loss after incineration at 550 °C. Total proteins were determined from the Kjeldahl technique. Extractable lipids were calculated according to the Soxhlet extraction method using a mix of 1:1 (v:v) of diethyl ether–petroleum ether as solvent. The sample mass of semolina was 5 g. The solvent–oil mixture was then evaporated using a rotary vacuum evaporator (Heidloph laboratora 4000) for 5 h at 40 °C and 40 rpm to recover pure oil. The boiling flask without solvent was dried in an oven at 100 °C for 1 h and the fat percentage was calculated by difference of weight. Finally, the carbohydrate content was determined by difference of totals. Tests were triplicated.

2.3. Particle size

The particle size distributions were determined using a laser granulometer (Mastersizer 2000 Malvern Instruments, UK) in dry and liquid mode. The Mastersizer 2000 uses high-pressure air to disperse and feed dry powder through the laser ray where the dispersion is controlled by adjusting the air pressure. The instrument is also equipped with a liquid sample dispersion module that is suited for powders in suspension. After dispersion of the powder, the particles diffract the laser, and the diffraction patterns are detected and the particle size is calculated. Five measurements were conducted with each powder sample. Most of the samples were analysed by air dispersion at 3.5 bars. Liquid dispersion was used only for low-quantity samples, where for each measurement approximately 0.25 g of the powder was dispersed in 75 ml of ethanol (to obtain a good obscuration and to avoid particles superposition).

2.4. Microscopy ESEM

The powders were observed with a Field-Emission Environmental Scanning Electron Microscope (ESEM FEG) (XL30, FEI/Philips, Netherlands) operating at 20 kV. High vacuum mode was used for raw and sieved semolina; low vacuum mode (1.4 Torr) was used for powders at different RHs. Powders were spread onto a double-sided adhesive carbon disc fixed on a support. Raw and sieved semolina were coated with platinum by a Polaron sputter coater (SC7640) and observed with a secondary electron (SE) detector. Powders at different RH were directly observed with a gaseous secondary electron (GSE) detector.

2.5. Dynamic vapour sorption

Sorption isotherms of powders were obtained with a Surface Measurement System Automated Dynamic Vapour Sorption (DVS1000) equipped with a controlled atmosphere microbalance. The experiments were carried out at constant temperature (25 °C) with different RH values ranging between 0% and 95%. Approximately 100 mg of powder was loaded onto the quartz sample pan. First, the samples were dehydrated in the DVS chamber (RH = 0%) for 60 min, and then the samples were submitted to a 10 step hydration process. The process was performed with 9 RH increments of 10% and a last step at 95% RH. The samples were considered to be at equilibrium when the value dm/dt (slope of the changing in mass with time) was set to be <0.005 mg min^{-1} or equilibration time exceeded 300 min.

G.A.B. (Guggenheim, Anderson and de Boer) and Y&N (Young and Nelson) equations were used to model experimental data. The quality of fit was evaluated by a linear correlation coefficient (R^2), where a value above 0.85 indicates an appropriate data model. Monolayer values as well as multilayer properties were calculated by GAB and Y&N models and then compared.

2.5.1. G.A.B.

G.A.B. model (Eq. (1)) is an extension of the Brunauer–Emmett–Teller (B.E.T.) equation. This model is widely used in food studies. It considers that the sorption heat of multilayers is different from the liquefaction heat. The equation was fitted to sorption isotherms from 0.1 to 0.8 a_w. In this equation (Eq. (1)), C is the Guggenheim constant, k is correcting constant involving multilayer properties and bulk liquid properties, X_w is the equilibrium moisture content expressed on dry matter (% dm), and X_m is the monolayer moisture content (% dm) [10].

$$X_w = \frac{X_m \cdot C \cdot k \cdot a_w}{[1-k \cdot a_w] \cdot [1 + (C-1) \cdot k \cdot a_w]} \quad (1)$$

2.5.2. Young and Nelson (Y&N)

Y&N is a model derived from the G.A.B. model, by considering that, in addition to surface binding forces, diffusional forces are also present, and these forces could become dominant when multi-molecular layers of water are present. In this case diffusional forces would be harder with the increment of water molecules at the surface. Finally, binding surface forces enable movement of water into the sample, which is the case for a lot of samples in food science. The experimental sorption and desorption data can be fitted to the following equations (Eqs. (2) and (3)):

$$M_S = A(\theta + \alpha) + B\varphi \quad (2)$$

$$M_D = A(\theta + \alpha) + B\theta \mathrm{RH}_{max}. \quad (3)$$

M_S and M_D are equilibrium moisture contents for the respective cycle at each relative humidity, and RH_{max} is the maximum exposed relative humidity. A and B are defined as:

$$A = \frac{\rho_w V_{ads}}{D} \quad (4)$$

$$B = \frac{\rho_w V_{abs}}{D} \quad (5)$$

ρ_W is the density of water at the experimental temperature; D is the sample dry weight, and V_{ads} and V_{abs} the volumes of adsorbed and absorbed water [11].

The parameters θ, α and φ in Eqs. (2) and (3) are related to an E term through the following expressions:

$$\theta = \frac{\mathrm{RH}}{\mathrm{RH} + (1-\mathrm{RH})E} \quad (6)$$

$$\alpha = -\frac{E\mathrm{RH}}{E-(E-1)\mathrm{RH}} + \frac{E^2}{(E-1)} \ln \frac{E-(E-1)\mathrm{RH}}{E} - (E+1)\ln(1-\mathrm{RH}) \quad (7)$$

$$\varphi = \theta \mathrm{RH} \quad (8)$$

$$E = e^{-\frac{q_1 - q_L}{k_B T}} \quad (9)$$

q_1 is the heat of adsorption of water bound to the surface of the sample, q_L is the heat of condensation of water molecules, k_B is Boltzmann's constant and T is the absolute temperature.

The experimental data is fitted to determine the values of *A*, *B* and *E* parameters.

2.5.3. Diffusion by Fick law

The diffusion coefficient of water vapour into semolina powder was obtained from Fick's second law (Eq. (10)), which can be used to calculate the diffusion in particles (Eq. (11)).

$$F = -D_f \cdot \frac{\delta c}{\delta x} \tag{10}$$

$$\frac{M_t}{M_{eq}} = 1 - \frac{6}{\pi^2} \sum_i w(a_i) \sum_{n=1}^{\infty} \frac{1}{n^2} \exp\left(\frac{-D \cdot n^2 \cdot \pi^2 \cdot t}{a_i^2}\right) \tag{11}$$

where M_t is the water content (kg of water/kg dm) at time t (min), M_{eq} is the water content (kg of water/kg dm) at equilibrium ($t = \infty$) a_i is the radius (m) of the particle i; $w(a_i)$ is the weight fraction of particles that are characterized by the radius; n is the calculation increment. At initial conditions the equation can be expressed:

$$M_t = \left(M_i - M_{eq}\right) - \frac{6}{\pi^2} \sum_i w(a_i) \sum_{n=1}^{\infty} \frac{1}{n^2} \exp\left(\frac{-D \cdot n^2 \cdot \pi^2 \cdot t}{a_i^2}\right) + M_e \tag{12}$$

where M_i is the water content at initial conditions ($t = 0$). Changes in sample mass ($\ln M_i - M_e$) are plotted as a function of hydration time, from which model parameters D, M_i, and M_e can then be calculated. Accuracy of the model was confirmed by regression coefficients values and residual errors.

The sphere model was often used to study water vapour sorption into food particles [5,12,13]. In our case, even if the semolina particles have an irregular angular shape, the sphere model was used. The calculation method of SMS was used here for the calculation of the water diffusion coefficient [14].

3. Results and discussion

3.1. Bulk composition

Table 1 shows the physicochemical bulk composition of raw and sieved semolina. Subtle but clear tendencies can be observed. A higher ash content is observed in fine powders (0–160 and 160–250 μm), which decreases when particle size increases. The protein and lipid contents increase with the increase of particle size. The increase is clearest for the case of lipids. Humidity does not differ greatly; values are in the same range for all the fractions except for 400–500 μm fraction which presents a lower value. Finally, carbohydrates are deduced by difference from the total, consequently, a lower value is obtained for 400–500 μm fraction. Wheat flours and semolina compositions were reported in literature, showing differences due to the nature and the origin of the material [4,5,15,16]. Similar results using fractioned semolina were reported by Hébrard et al. [4]. However these authors found the opposite tendency for protein and lipid content, where there was a decrease with the increase of the particle size. This difference may be attributed to the different particle size fraction ranges they used, or also to the nature of raw material. Taking into account the standard deviation of the values obtained, it can be observed that there is no significant difference in the principal components of the fractions (proteins, lipids and carbohydrates), which means that the possible differences in sorption properties and water diffusion coefficients may be attributed to only the differences in particle size.

3.2. Effect of water uptake on powder structure and particle size

3.2.1. Particle structure

Fractions 0–160, 250–315 and 400–500 μm were held in saturated atmospheres for 7 days, allowing water exchange between powder and relative humidity of the atmosphere. Powders *pseudo*-equilibrated at 75, 85 and 97% RH were observed by ESEM. The images shown in Fig. 1 at 50× show that the powders conserved the same structure up to 85% RH, then agglomeration takes place at 97% RH. This agglomeration was clearest in finest particles. At 800×, the morphology of surfaces at 75% RH is not really affected in comparison with initial powders. Some modifications on the protein matrix could be observed at 85%RH and became clear at 97% RH. Indeed, the hard structure of protein changed into a softer matter, and then bridges were formed among particles producing agglomeration. The gluten–starch bond is really strong, but can be easily separated with water [17]. Consequently the modification of the protein matrix caused the exposure of starch grains, interacting directly with humidity. The starch texture did not change, but starch grains swelled. Pure wheat starch swelled to 17% of its initial volume due to humidity [18]. The percentage value of this swelling depends on the complexity of the protein–starch matrix; however an increase of the grain size is clear. This evolution of the microstructure becomes more evident at high RH. As specific surface is inversely proportional to the particle size, a greater water uptake is seen in small particles, which have a smaller particle volume, consequently the same quantity of water wets the particle deeper; thus the formation of bridges between particles is observed. On the other hand, big particles uptake a smaller quantity of water, consequently the formation of bridges leading to obtaining granulates is more difficult. Another interesting observation is the number of broken starch grains that can be easily observed at 97% RH. This provides evidence that the finest particles (0–160 μm) suffered a rupture at the gluten–starch bond edge. These particles are naturally detached from the bigger particles during milling, whereas bigger particles present fractures at the starch grains. These fractures are the result of a difficult breaking of the gluten–starch bond, produced by blades during milling of the wheat kernel [6]. The resistance to the separation of the starch–protein binding is characteristic of hard flours [17]. This evolution of the structure can be related to the heterogeneity of the kernel texture. Another possibility is the milling conditions applied to the grain kernel. Saad et al. proposed that milling conditions could apply different forces throughout the grain and produce two kinds of ruptures: grains broken at the edge and grains broken through the starch particle [15].

3.2.2. Particle size

The particle size of 0–160, 250–315 and 400–500 μm fractions after conditioning at different RH at 25 °C is shown in Table 2. The size evolution of 0–160 μm particles was not significant at low RH (11 and 54%),

Table 1
Particle size (dry dispersion) and bulk chemical composition (g/100 g dm).

Fractions	D(50) μm	Ashes	Proteins	Lipids	Humidity	Total	Carb.[a]
Raw semolina	298.31	0.91 ± 0.02	11.51 ± 0.36	1.52 ± 0.26	12.99 ± 0.05	26.93	73.07
0–160 μm	135.65	1.36 ± 0.03	10.62 ± 0.35	0.92 ± 0.18	12.40 ± 0.05	25.30	74.70
160–250 μm	218.67	0.94 ± 0.02	11.04 ± 0.20	0.97 ± 0.21	12.63 ± 0.02	25.58	74.42
250–315 μm	288.36	0.76 ± 0.01	11.05 ± 0.73	1.25 ± 0.12	12.21 ± 0.01	25.27	74.73
315–400 μm	373.76	0.70 ± 0.02	11.13 ± 0.34	1.16 ± 0.13	12.88 ± 0.14	25.87	74.13
400–500 μm	438.96	0.70 ± 0.03	11.92 ± 0.61	1.73 ± 0.22	11.76 ± 0.00	26.11	73.89

[a] Carbohydrates are calculated by difference from the total.

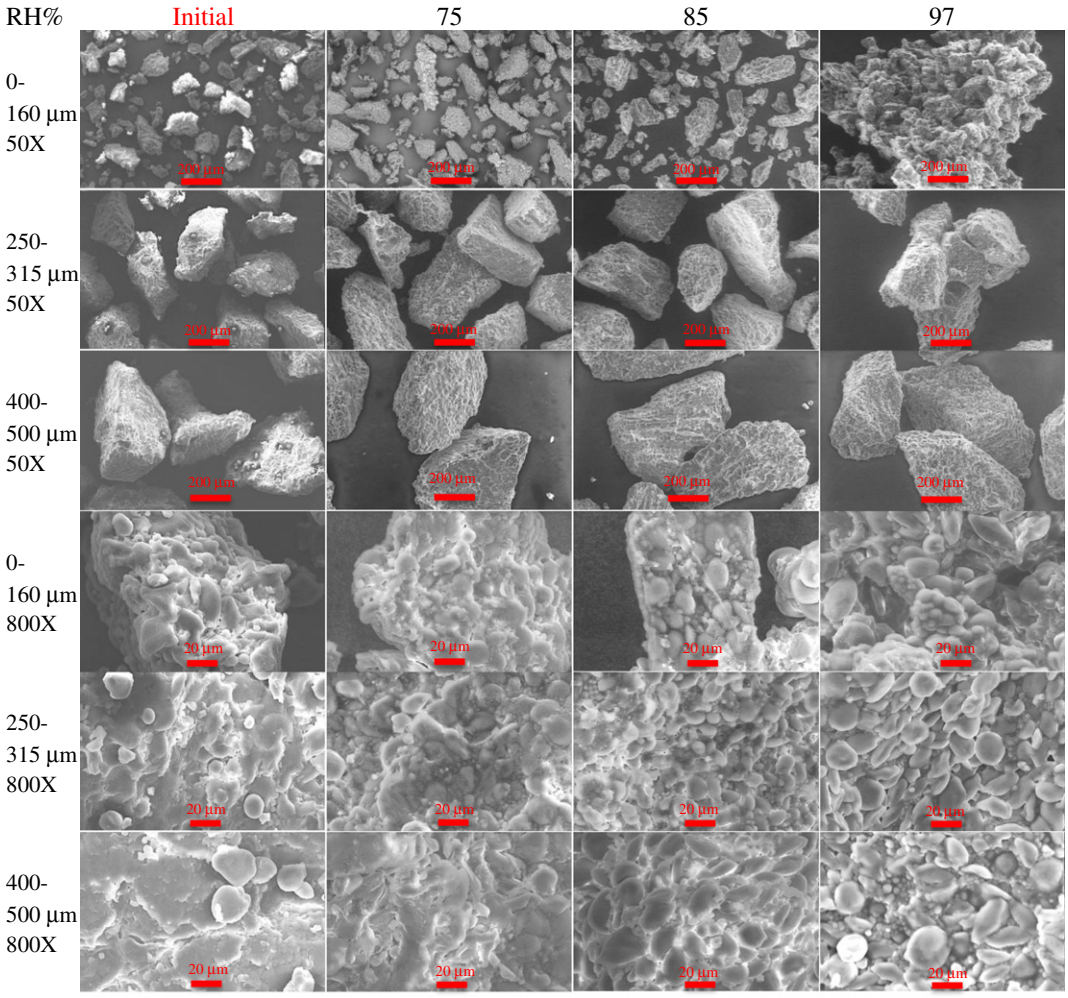

Fig. 1. ESEM images at 50 and 800× of sieved semolina particles (0–160, 250–315 and 400–500 µm) conditioned at different RHs at 25 °C.

but an increase of a few microns was registered at 75% RH and 85% RH. Finally, a large increase in particle size was observed at 97% RH, corresponding to the agglomeration of the particles. The 250–315 µm fraction presented an evolution in size between 11 and 54% RH but remained constant at 75% RH. A more considerable gain was observed at 85% RH and at 97% RH. Finally, particles from 400 to 500 µm fraction showed the highest evolution in size, around 10 µm with the first steps (11,54, 75, 85 and 97%). However, at 97% RH the size gain is nor as much as for 0–160 and 250–315 fractions, indicating a reduced or non-existent agglomeration. The increase in particle size is observed below 85% RH whereas agglomeration is observed above 97%RH as a drastic increase of the particle size. The agglomeration phenomenon is clearest for small particles. After 7 days, the water diffusion was probably not enough to shift equilibrium at 100%. In fact a *pseudo*-equilibrium was preferred since a longer duration of the experiment would have generated the presence of microorganisms. Consequently as shown in Table 3, the water uptake is similar for all the fractions. Since all fractions have an increased water uptake, the measure of particle size after conditioning of the fractions can be considered equal for all the particles. The diffusion coefficient was calculated from this new D_{50} value.

3.3. Sorption isotherm

Fig. 2 shows a type II sorption isotherm curve according to the IUPAC classification which is characteristic of finely divided non-porous solids or macro-porous materials [17]. Three zones in the curve are observed I (0–20% RH), II (20–80% RH) and III (80–95% RH). Zone I represents the monolayer formation; zone II corresponds to the linear portion of the isotherm where the added water will bind with the components

Table 2
Particle size (liquid dispersion) after 7 days at different RHs at 25 °C.

	RH%	D(50) µm		
		0–160 µm	250–315 µm	400–500 µm
Initial	–	105.60 ± 1.03	329.43 ± 6.24	546.71 ± 5.62
LiCl	11	103.53 ± 0.87	321.89 ± 4.70	525.78 ± 9.54
$MgNO_2$	54	101.30 ± 1.24	327.74 ± 4.75	539.08 ± 4.83
NaCl	75	112.02 ± 1.23	328.71 ± 2.25	543.38 ± 9.32
KCl	85	117.89 ± 2.12	335.20 ± 2.88	553.77 ± 10.69
K_2SO_4	97	531.30 ± 46.42	386.07 ± 12.41	581.43 ± 12.79

Table 3
Water taken by powders after 7 days at different RHs at 25 °C.

RH%	Water taken %		
	0–160 µm	250–315 µm	400–500 µm
11	−5.90 ± 0.2	−7.30 ± 0.1	−6.70 ± 0.3
54	0.24 ± 0.0	0.17 ± 0.2	0.30 ± 0.2
75	2.82 ± 0.1	2.86 ± 0.5	2.27 ± 0.8
85	7.20 ± 0.8	6.40 ± 0.8	7.67 ± 1.0
97	25.03 ± 2.9	24.19 ± 3.0	25.15 ± 3.6

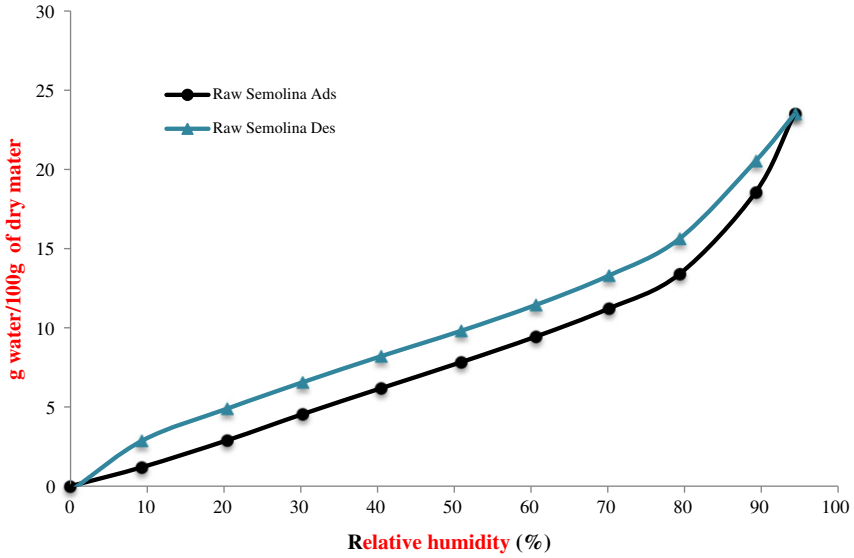

Fig. 2. Isotherm of raw semolina (absorption and desorption) at 25 °C.

of the material forming layers. In zone III, water presents weak binding. In this state water is mobile. The "S" curve with hysteresis after desorption is classical behaviour of natural high molecular weight polymers [1,4].

The same II type curve is observed in the isotherms of the different size fractions (Fig. 3), which display differences in the mass of water absorbed. Between 20 and 80% RH, the curves were parallel and there is no difference in the absorption of water. Nevertheless, from 0 to 20% RH, values decreased with the increase in particle size. This means that fine particles absorb more water. Similar curves have been reported elsewhere for hard flours [1,3,4,16].

Differences in mass gain with particle size increment can be due to a bigger contact surface offered by small particles. Raw semolina (not plotted in Fig. 3) appeared at the centre as an average of all the curves.

3.4. G.A.B.. and Y&N models

3.4.1. GAB

Coefficients calculated from GAB model (Eq.(1)), are expressed in Table 4. This model presented a good correlation; r_{GAB} values are over 0.99 (for 0.5 > HR > 80 as recommended by UPAC) for all the samples. The GAB model has a limit ($0 < K_{GAB} \leq 1$) imposed by the physics behind GAB equation (Eq.(1)). This limit was respected for all the powders. All values are consistent with those observed by Hébrard et al. [4]. The monolayer values are similar for all the fractions, which mean that the water content to saturate the monolayer is independent of the particle size. K_{GAB} represents the multilayer moisture capacity, similar interactions were found for all the powders. C_{GAB} denotes the interaction with the surface; a larger interaction was registered by 0–160 μm, which can be explained by a bigger specific surface offered by the finest particles. X_m, C_{GAB} and K_{GAB} values for all the powders are consistent with Hébrard et al. [4] on semolina and other studies with wheat products [19].

3.4.2. Young and Nelson (Y&N)

The Y&N model showed good correlation with the experimental data for all the fractions (Table 4). A correlation coefficient $R^2_{Y\&N} > 0.99$ was observed for all the fractions, which prove a correct fit of the Y&N equation to the experimental data (for 0 > HR > 90 a longer range than GAB). $A_{Y\&N}$ is equivalent to X_m in the GAB equation and represents the moisture capacity of a monomolecular layer; $B_{Y\&N}$ is related to the amount of moisture absorbed by the sample and there is no similar term in the GAB model. Finally, $E_{Y\&N}$ is an energy term relating the strength of water vapour interaction to the surface of the sample. This term is similar

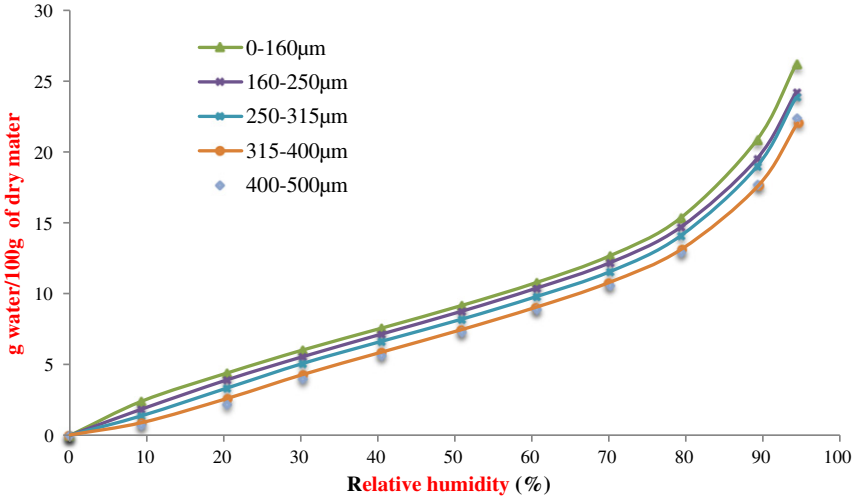

Fig. 3. Isotherm of semolina fractions (absorption) at 25 °C.

Table 4
Equation parameters by GAB and Y&N models.

Semolina	G.A.B..				Y&N			
	X_m (kg/kg dm)	C_{GAB}	K_{GAB}	R^2_{GAB}	$A_{Y\&N}$ (kg/kg dm)	$E_{Y\&N}$	$B_{Y\&N}$ (kg/kg dm)	$R^2_{Y\&N}$
Raw	0.08	7.21	0.68	0.99	0.03	0.48	0.06	0.99
0–160 μm	0.09	10.63	0.64	0.99	0.04	0.26	0.04	0.99
160–250 μm	0.08	4.20	0.63	0.99	0.04	0.31	0.05	0.99
250–315 μm	0.07	4.20	0.70	0.99	0.03	0.40	0.06	0.99
315–400 μm	0.07	4.18	0.71	0.99	0.03	0.54	0.07	0.99
400–500 μm	0.10	4.74	0.58	0.99	0.03	0.58	0.08	0.99

to C_{GAB}. The monolayer values present the same tendency as the GAB calculation. However a lower value is observed. The difference is due to the model, which, in effect, is considered a monolayer with a lesser quantity of water molecules. The rest of the humidity is taken into account in the $B_{Y\&N}$ parameter as absorbed water. The moisture absorbed by the particle ($B_{Y\&N}$) increases with the increase in particle size. This largest volume of absorbed water can be attributed to a bigger particle volume. Finally, $E_{Y\&N}$ increases with the particle size. This last parameter indicates a stronger interaction between water vapour and the surface of the biggest particles.

3.5. Water diffusion coefficient

Water diffusivity in semolina was calculated for each RH level from water sorption kinetic curves. One example of the curve is shown in Fig. 4 The water diffusion coefficients of raw semolina and various size fractions can be obtained by applying Fick's law for spherical particles (Eq. (11)). Calculations were done with D(50) obtained by dry dispersion. The correlation coefficient for each HR, in all the samples, was over 0.99, which indicates that Fick's equation does give a good fit to experimental data. Curves of the diffusion coefficients as a function of the HR are presented in Fig. 5. A similar bell-like curve was found for a film of semolina [7], as for hydrophilic porous samples such as cereal-based products [20–22]. This behaviour is due to the change in mechanism from vapour diffusion at low RH into liquid diffusion at high RH, producing an evolution of the material's porosity and microstructure. For Guillard et al. diffusivity variations were correlated with the changes in microstructure of the material that was observed by using environmental scanning electron microscopy [20]. In the case of semolina, these changes in the microstructure and inter and intra-porosity were also observed in SEM pictures (Fig. 1).

A trend was observed in Fig. 5, where the diffusion is directly proportional to the particle size. The water diffusion coefficients at HR = 90% for the fractions are 0.56, 0.53, 0.96, 1.54 and 3.36 for fractions 0–160, 160–250, 250–315, 315–400 and 400–500 μm respectively. These results revealed an interesting correlation of the particle size with the water diffusion. For large particles (315–400 and 400–500 μm fractions) the diffusion was fast until a monolayer (10% RH) is formed. Then a deceleration of diffusion was observed from 10 to 30% RH, after which a new acceleration was observed, registering the highest rate at 60% RH. Finally, at saturation humidity, the speed was reduced progressively. On the other hand, with small particles (0–160, 160–250 and 250–315 μm fractions) the diffusion starts slowly until a monolayer (10% RH) is formed, and a progressive acceleration is seen up to a maximal rate observed at 40% RH. Then at saturation humidity the rate progressively decreases. Raw powder has a curve, which is the resultant of the influence of the behaviours of all the fraction, bringing into evidence the effect of the particle size in the water diffusion coefficient.

3.6. Dynamic water diffusion coefficient

Water diffusion coefficients where re-calculated by taking into account the evolution of particle size produced by static water vapour sorption of samples (0–160, 250–315, and 400–500 μm). The diameter of fractions obtained after conditioning at 11, 54, 75, 85 and 97% RH was used to re-calculate water diffusion coefficients at 10, 50, 70, 80 and 95% coefficients using DVS data. These new coefficients are referred to in this text as dynamic water diffusion coefficients. Initial and dynamic diffusion coefficients are shown in Table 5. Curves of both diffusion coefficients are shown in Fig. 6. The diffusion coefficient of each fraction is not greatly affected by change in particle size. As a consequence of the swelling of the particles by water uptake, there is little diminution of

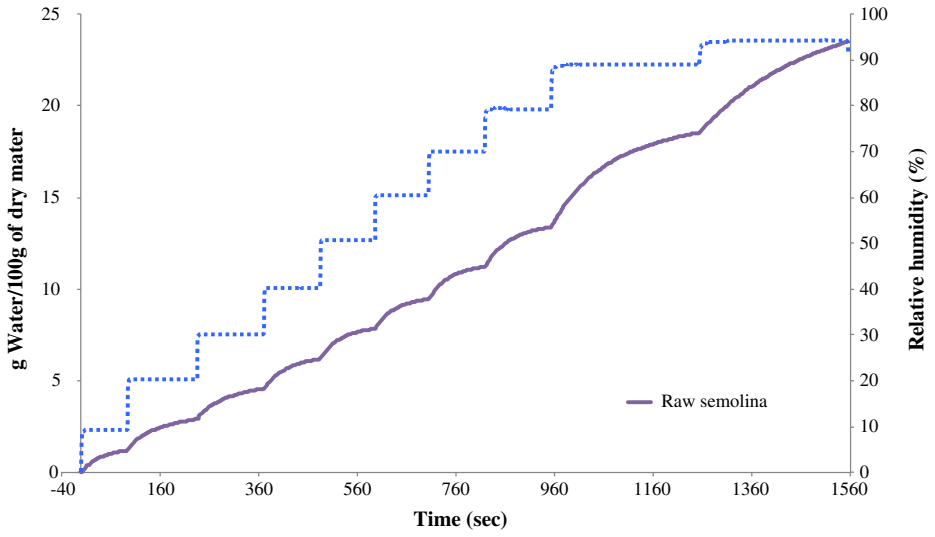

Fig. 4. Example of kinetic data obtained during water adsorption of raw semolina at 25 °C and measured by DVS automatic sorption analyzer.

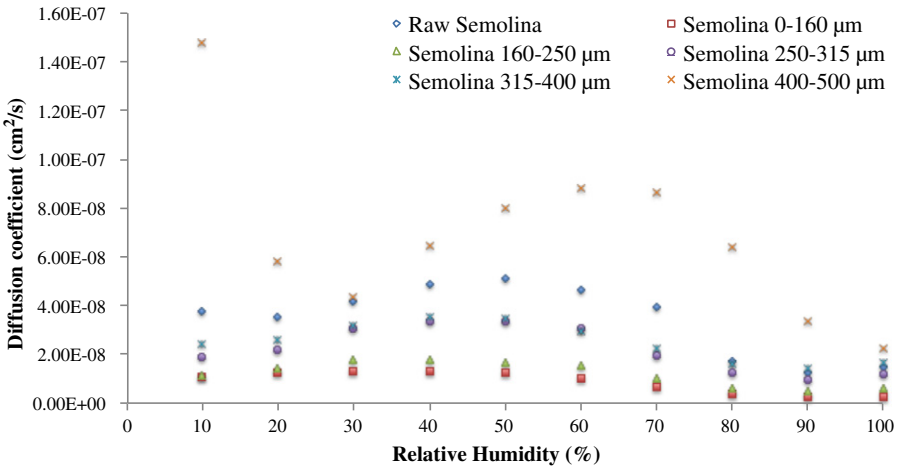

Fig. 5. Influence of particle size on water diffusion coefficient.

Table 5
Water diffusion coefficients.

RH%	Diffusion coefficient (cm^2/s)						
	Raw	0–160 µm		250–315 µm		400–500 µm	
	Initial	Initial	Dynamic	Initial	Dynamic	Initial	Dynamic
10	3.78E−08	1.10E−08	1.08E−08	1.92E−08	1.71E−08	14.8E−08	13.1E−08
50	5.14E−08	1.26E−08	1.20E−08	3.39E−08	3.05E−08	8.01E−08	7.67E−08
70	3.93E−08	0.67E−08	0.74E−08	1.98E−08	1.81E−08	8.64E−08	8.47E−08
80	1.75E−08	0.37E−08	0.46E−08	1.25E−08	1.52E−08	6.43E−08	6.70E−08
90	1.26E−08	0.26E−08	3.73E−08	0.97E−08	1.46E−08	3.36E−08	3.86E−08

rate at the initial points (10% RH). Only the 0–160 fraction at 95%HR increased drastically, due to a clear agglomeration of the particles.

A similar dynamic water diffusion coefficient was determined for milk powders [8]. In this case, the evolution of the water diffusion coefficient was largely affected by particle size and particle structure. The differences in the evolution of the particle size and consequently on the dynamic water diffusion coefficient are probably due to the different nature of the components. For example, lactose presents crystallization at 54%RH having an effect in the particle size. Lactose as well as milk proteins are soluble. In the case of semolina, initial and dynamic water diffusion coefficients do not show big differences in the evolution of the curves, which can be explained by a non-soluble and stable structure in the presence of water. Indeed, the structure of semolina particles will be affected only at very large RH (>95%).

4. Conclusion

Water diffusion was studied in raw and 5-fractions of sieved semolina coupled with the microstructure and composition properties. The differences observed are related to the particle size through the specific surface and the evolution of the protein matrix due to moisture diffusion. At high RH the protein matrix changes its structure allowing the formation of bridges, causing agglomeration. Such agglomeration was most evident on small particles where the starch grains showed an

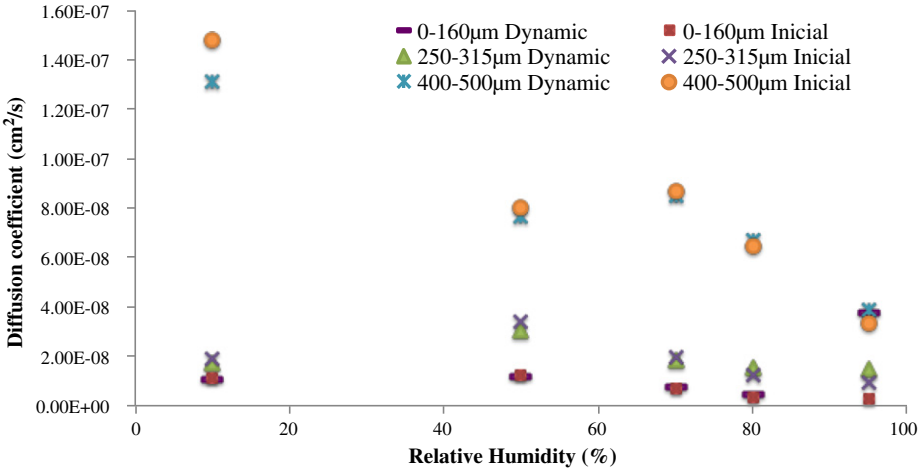

Fig. 6. Initial and dynamic water diffusion coefficients.

evolution in size. The Y&N model considers the absorption of water, which corresponds better with the nature of food powders, and with the evolution of the microstructure in the presence of moisture observed by ESEM. Both particle sorption properties and water diffusion are affected by particle size. In fact, the smallest particles show a greater water adsorption and a slower water diffusion coefficient. The values are proportional and evolve with the particle size. This behaviour can be explained by the specific surface which is inversely proportional to the particle size thus small particles have the larger specific surface. Water diffusion coefficients were not affected by size evolution of semolina particles due to the non-soluble properties of samples. Changes were produced by hydration (>95%HR) and not by humidification (<95%HR). In the future, knowledge of these factors can be used to better control powder hydration as well as the agglomeration mechanism in both production and storage conditions.

Acknowledgements

ANR funding from program "Reactive Powder" is gratefully thanked. Christine Rolland is also thanked for support in the use of ESEM. In addition, first author acknowledges the National Research Association (ANR) in France, the Mexican National Council of Science and Technology (Consejo Nacional de Ciencia y Tecnología, CONACYT) and the Complementary Scolarships of SEP in Mexico (Becas complemento SEP) for financial resources.

References

[1] W. Bushuk, C.A. Winkler, Sorption of water vapour on wheat flour, starch and gluten, Cereal Chem. 34 (1957) 73–86.
[2] C.J. Lomauro, A.S. Bakshi, T.P. Labuza, Moisture transfer properties of dry and semi-moist foods, J. Food Sci. 50 (1985) 397–400.
[3] K.A. Riganakos, P.G. Demertzis, M.G. Kontominas, Study of water sorption of flours (wheat and soy) using a hygrometric method: effect of relative humidity during heat treatment, Z. Lebensm. Unters. Forsch. A. 204 (1997) 369–373.
[4] A. Hébrard, D. Oulahna, L. Galet, B. Cuq, J. Abecassis, J. Fages, Hydration properties of durum wheat semolina: influence of particle size and temperature, Powder Technol. 130 (2003) 211–218.
[5] A.D. Roman-Gutierrez, F. Mabille, S. Guilbert, B. Cuq, Contribution of specific flour components to water vapor adsorption properties of wheat flours, Cereal Chem. 80 (2003) 558–563.
[6] M. Saad, C. Gaiani, J. Scher, B. Cuq, J.J. Ehrhardt, S. Desobry, Impact of re-grinding on hydration properties and surface composition of wheat flour, J. Cereal Sci. 49 (2009) 134–140.
[7] D. Oulahna, A. Hebrard, B. Cuq, J. Abecassis, J. Fages, Agglomeration of durum wheat semolina: thermodynamic approaches for hydration properties measurements, J. Food Eng. 109 (2012) 619–626.
[8] I. Murrieta-Pazos, C. Gaiani, L. Galet, B. Cuq, S. Desobry, J. Scher, Comparative study of particle structure evolution during water sorption: skim and whole milk powders, Colloids Surf. B 87 (2011) 1–10.
[9] R.E. Wrolstad, E.A. Decker, S.J. Schwartz, P. Sporns, E.A. Decker, S.J. Schwartz, Handbook of Food Analytical Chemistry, Water, Proteins, Enzymes, Lipids, and Carbohydrates, 1.a ed. Wiley-Interscience, 2004.
[10] N.H. Dural, A.L. Hines, Adsorption of water on cereal–bread type dietary fibers, J. Food Eng. 20 (1993) 17–43.
[11] M.E. Lyn, D. Burnett, A.R. Garcia, R. Gray, Interaction of water with three granular biopesticide formulations, J. Agric. Food Chem. 58 (2010) 1804–1814.
[12] H.A. Becker, A study of diffusion in solids of arbitrary shape, with application to the drying of the wheat kernel, J. Appl. Polym. Sci. 1 (1959) 212–226.
[13] X. Yu, A.R. Schmidt, L.A. Bello-Perez, S.J. Schmidt, Determination of the bulk moisture diffusion coefficient for corn starch using an automated water sorption instrument, J. Agric. Food Chem. 56 (2008) 50–58.
[14] D. Burnett and F. Thielman, Calculation of diffusion constants in a pharmaceutical powder using DVS, Application note 30, Surface Measurement Systems Ltd.
[15] M. Saad, C. Gaiani, M. Mullet, J. Scher, B. Cuq, X-ray photoelectron spectroscopy for wheat powders: measurement of surface chemical composition, J. Agric. Food Chem. 59 (2011) 1527–1540.
[16] A. Ocieczek, Comparison of sorption properties of semolina and farina, Acta Agrophysica. 9 (2007) 135–145.
[17] J.A. Delcour, R.C. Hoseney, Principles of Cereal Science and Technology, Third Edition, 3.a ed., Am. Assoc. Cereal Chem., 2010.
[18] F. El-Khawas, R. Tawashi, H. Von Czetsch Lindenwald, Water vapor sorption and suction potential of starch grains, J. Soc. Cosmet. Chem. 17 (1966) 103–114.
[19] M. Lagoudaki, P.G. Demertzis, Equilibrium moisture characteristics of food — hysteresis effects and isotherm models, Lebensmittal-Technol. 26 (1993) 71–77.
[20] V. Guillard, B. Broyart, C. Bonazzi, S. Guilbert, N. Gontard, Moisture diffusivity in sponge cake as related to porous structure evaluation and moisture content, J. Food Sci. 68 (2003) 555–562.
[21] E. Roca, B. Broyart, V. Guillard, S. Guilbert, N. Gontard, Controlling moisture transport in a cereal porous product by modification of structural or formulation parameters, Food Res. Int. 40 (2007) 461–469.
[22] F. Chivrac, H. Angellier-Coussy, V. Guillard, E. Pollet, L. Avérous, How does water diffuse in starch/montmorillonite nano-biocomposite materials? Carbohydr. Polym. 82 (2010) 128–135.